

Contents lists available at [ScienceDirect](https://www.sciencedirect.com)

Journal of Rock Mechanics and Geotechnical Engineering

journal homepage: www.jrmge.cn

Full Length Article

Effects of synthetic site water on bentonite-concrete system for a potential nuclear waste repository

Zhao Sun ^{a, b}, Yong-Gui Chen ^{a, *}, Wei-Min Ye ^a, Qiong Wang ^a, Dong-Bei Wu ^c, Zhen-Yu Yin ^b

^a Key Laboratory of Geotechnical and Underground Engineering of Ministry of Education, Department of Geotechnical Engineering, Tongji University, Shanghai, 200092, China

^b Department of Civil and Environmental Engineering, The Hong Kong Polytechnic University, Hung Hom, Kowloon, Hong Kong, China

^c School of Chemical Science and Engineering, Tongji University, Shanghai, 200092, China



ARTICLE INFO

Article history:

Received 5 July 2023

Received in revised form

26 December 2023

Accepted 20 January 2024

Available online 14 June 2024

Keywords:

Mock-up device

GMZ bentonite

Site water-concrete-bentonite system

Geochemistry

Buffer performance

ABSTRACT

In high-level nuclear waste (HLW) repositories, concrete and compacted bentonite are designed to be employed as buffer materials, which may raise a problem of interactions between concrete and bentonite. These interactions would lead to mineralogy transformation and buffer performance decay of bentonite under the near field environment conditions in a repository. A small-scale experimental setup was established to simulate the concrete-bentonite-site water interaction system from a potential nuclear waste repository in China. Three types of mortars were prepared to correspond to the concrete at different degradation states. The results permit the determination of the following: (1) The macro-properties of Gaomiaozi (GMZ) bentonite (e.g. swelling pressure, permeability, the final dry density, and water content of reacted samples); (2) The composition evolution of fluids from the synthetic site water-concrete-bentonite interaction systems; (3) The sample characterization including Fourier transform infrared spectroscopy (FTIR) and X-ray powder diffraction (XRD). Under the infiltration of the synthesis Beishan site water (BSW), the swelling pressure of bentonite decreases slowly with time after reaching its second swelling peak. The flux decreases with time during the infiltrations, and it tends to be stable after more than 120 d. Due to the cation exchange reactions in the BSW-concrete-bentonite systems, the divalent cations (Ca and Mg) were consumed, and the monovalent cations (Na and K) were released. The dissolution of minerals in the bentonite such as albite causes Si increasing in the pore water. It was concluded that the hydro-mechanical property degradation of bentonite takes place when it comes into contact with concrete mortar, even under low-pH groundwater conditions. The soil dispersion, the uneven water content, and the uneven dry density in bentonite samples may partly contribute to the swelling decay of bentonite. Therefore, the direct contact with concrete has an obvious effect on the performance of bentonite.

© 2024 Institute of Rock and Soil Mechanics, Chinese Academy of Sciences. Production and hosting by Elsevier B.V. This is an open access article under the CC BY-NC-ND license (<http://creativecommons.org/licenses/by-nc-nd/4.0/>).

1. Introduction

The advent of nuclear energy has prompted concerns about the safe disposal of high-level nuclear wastes (HLW). It is accepted that the most reasonable way to dispose of the HLW is to build a multi-barrier system in deep repositories (Villar and Lloret, 2008; Ye et al.,

2010). The long-term safety of nuclear waste repositories is a geological problem faced by all countries with nuclear technology. Bentonite and concrete are selected as important components of the multi-barrier system in disposal (Pusch, 1979; Karnland et al., 2007). Bentonite, due to its inherent material advantages, plays an important role in the physical and chemical security around nuclear waste canisters, such as blocking the migration of nuclides and providing mechanical support. On the other hand, concrete or cement materials are often used in large quantities to reinforce the surrounding rock and block the groundwater (Glasser 2001; Liu et al., 2023). During the long-time storage of the repository, the

* Corresponding author.

E-mail address: cyg@tongji.edu.cn (Y.-G. Chen).

Peer review under responsibility of Institute of Rock and Soil Mechanics, Chinese Academy of Sciences.

concrete would suffer from the infiltration of site water. As a result, the cement degrades with time (Savage, 1997; Nakayama et al., 2004; Fernández et al., 2006; Lehtikoinen, 2009). It has been reported that for ordinary Portland cement (OPC), the cement degradation can be differentiated into three stages, releasing Na^+ , K^+ , and OH^- in the first stage, and then Ca^{2+} and OH^- in the second stage (e.g. Berner, 1992; Glasser and Atkins, 1994; Faucon et al., 1998; Fernández et al., 2010). The main characteristics of cement degradation are shown in Fig. 1.

It is calculated that the first degradation stage may persist for approximately 10,000 years from the beginning of cement degradation, and the second stage will last for a long period from 10,000 years to 200,000 years estimated by Heath and Hunter (2012) and Mon et al. (2017). It would be an ongoing, long-term process during which the alkaline compositions are released from cement to the site water and then inject into bentonites. It will induce complex interactions in the site water-concrete-bentonite system, raising scientific problems, for example, the impact of concrete degradation on the barrier performance of bentonite, which is an inevitable security problem in repository occurring in around 500 years to 100,000 years.

In terms of the long-term reaction of the concrete/bentonite interface, the mock-up test is the most effective way to investigate the effect of concrete degradation on bentonite. Some related researches have been performed focusing on the mineralogy evolution in bentonite impacted by concrete or cement degradation (e.g. Fernández et al., 2006, 2017; Dauzeres et al., 2010, 2016; Dolder et al., 2014; Lalan et al., 2016; Balmer et al., 2017). Meyer and Herbert (1999) carried out column tests in which cement blocks were put in contact with the bentonite blocks under different temperature and pH conditions. Calcium silicate hydrate (C–S–H) colloid, analcite, and magnesium clay minerals were found as the neoformations emerging at the cement/bentonite interface. A concrete (OPC mortar)/bentonite reaction chamber was employed for testing with the compacted bentonite of 1.4 Mg/m^3 dry density from La Serrata (Spain) in Fernández et al. (2006). The saturated $\text{Ca}(\text{OH})_2$ solution and 0.25 mol/L NaOH solution were injected into the concrete/bentonite system at 25°C , 60°C , and 120°C . The results show that $\text{Ca}(\text{OH})_2$ fluids failed to alter the bentonite mineralogy over the experiment time scale and a tobermorite layer of 1.5 mm formed in the clay side near the interface after the infiltration of NaOH solution at 120°C . Dauzeres et al. (2010) carried out

experiments on a confined clay/cement system with the pore water of $\text{pH } 7.1$ at 25°C for 2 months, 6 months, and 12 months. Results indicate that the degraded zone of cement (about $800 \mu\text{m}$) is composed of ettringite and C–S–H at $\text{pH } 10\text{--}11$ after 12 months of interactions. Additionally, it was found that the potassium fluid induces an illite enrichment within illite/smectite interstratifications. Cuevas et al. (2013, 2016) obtained pieces of evidence on the physical and geochemical processes occurring in FEBEX bentonite with a nominal dry density of 1.65 Mg/m^3 impacted by cementitious materials in the mock-up study. The tests were performed in cylindrical cells for 18 months at 60°C . Results supply that long-term modified bentonite can be collapsed by K-substituted smectite. Cation exchange reactions take place in bentonite on the interface, characterized by a complete replacement of Mg and a predominance of Ca and K. Besides, the porosity near the bentonite-mortar interface decreases. Dauzeres et al. (2016) studied the interaction of two different low-pH cements with Opalinus Clay at the Mont-Terri rock laboratory. Scanning electron microscopy with energy-dispersive X-ray spectroscopy (SEM-EDS) analyses presented that an Mg-enriched zone associated with the decalcification of C–S–H near the clay side was found after 2.5 years and 5 years. In both two cements, the zone extends up to 2–4 mm depth. Transmission electron microscopy and energy-dispersive X-ray spectroscopy (TEM-EDS) investigations also indicate that the formed Mg phase exhibits a gel-like structure. Balmer et al. (2017) performed small-scale mock-up tests on bentonite-iron and bentonite-cement systems to study the performance of bentonite close to the interfaces, taking the appropriate proportions of cement, bentonite, and iron in the repository into consideration. Data show the drop in cation exchange capacity (CEC) in the bentonite after the tests (Balmer et al., 2017; Kaufhold et al., 2020).

At present, there are many qualitative research results and few quantitative analyses, and the quantitative analysis mainly focuses on the mineralogy alteration of bentonite or clay minerals. For concrete/bentonite systems, the research is quite limited with more specific and meaningful results expected: (1) The evolution of bentonite macro-property influenced by the concrete under the injection of fluids; (2) The interaction of site water-concrete-bentonite system. To achieve these research targets, a small mock-up device was designed. Three types of mortar were prepared to simulate the concrete at three degradation stages corresponding to the young, middle, and evolved concrete. In China, Beishan in Gansu province eventually became the best choice of HLW disposal site with its advantages on account of a nationwide survey (Guo et al., 2010; Ye et al., 2010). This work tries to investigate the long-term interaction of synthetic Beishan site water (BSW)-concrete-compacted Gaomiaozi (GMZ) bentonite to simulate a potential case in Chinese nuclear waste repository. The results on the swelling pressure, the permeability, the composition evolution of infiltration water, and the sample characters were observed for further predicting the long-term bentonite barrier impacted by cement in a repository.

2. Material and experiments

2.1. Materials

2.1.1. Bentonite

The raw GMZ bentonite was extracted from Inner Mongolia of China, 300 km northwest of Beijing. It has a grain size of no more than $200 \mu\text{m}$ diameter (Sun et al., 2018) with the basic physical and chemical properties of GMZ bentonite listed in Table 1 (Qian, 2007). The bulk composition (mass fraction) of the sample used in this work was determined as follows: 58% montmorillonite, 21% quartz,

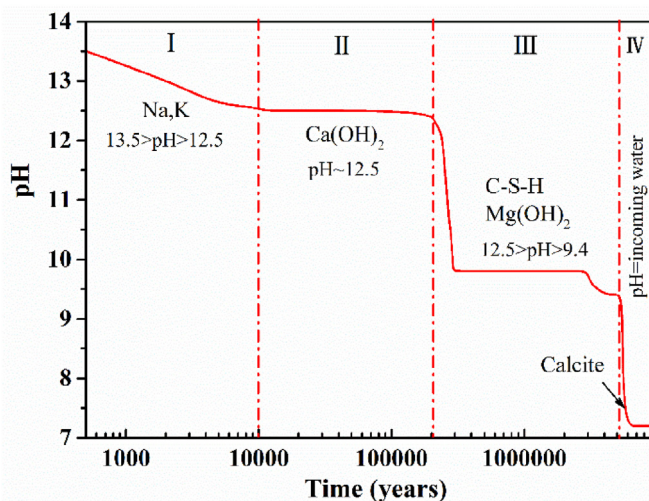


Fig. 1. Alkaline pore water pH and major solute changes due to cement degradation (adapted from Heath and Hunter, 2012; Mon et al., 2017).

Table 1
Some basic properties of the GMZ01 bentonite.

| Properties | Value |
|--|---|
| Specific gravity | 2.66 |
| pH | 8.68–9.86 |
| Total specific surface area (m ² /g) | 597 |
| BET specific surface area (m ² /g) ^a | 22.8 |
| CEC (cmol(+)/kg) | Na ⁺ 34.7, Ca ²⁺ 22.9, Mg ²⁺ 11.5, K ⁺ 0.56, total 76 |

^a BET-calculated by Brunauer-Emmett-Teller (BET) method.

6% cristobalite, 7% microcline, 8% albite, etc.

2.1.2. Concrete

In order to simulate the concrete at different degradation stages, the concrete mortar at three degradation stages was arranged according to the composition of the young, middle, and evolved stages of concrete. The OPC, quicklime, and quartz sand were adopted in the preparation of cement mortar or lime mortar according to the methods from Cuevas et al. (2013) with their specific ratio shown in Table 2. The formula determination is in accordance with: (1) The permeability of concrete mortar is much greater than that of bentonite, which is convenient for pore water entering into bentonite after full contact with concrete; (2) The hardened concrete has enough strength to ensure that it would not crack during the swelling of bentonite. The quicklime grade is analytic purity, and the size of quartz sand is about 40 mesh (Cuevas et al., 2013).

2.1.3. Synthetic site water

According to the geological and hydro-geological surveys, the main cations of groundwater in the Beishan area include Na⁺, K⁺, Ca²⁺, and Mg²⁺, and the main anionic compositions are Cl⁻ and SO₄²⁻ (Guo et al., 2001). The BSW is prepared with sulfates and chlorides to simulate the groundwater conditions in the potential Chinese repository. The compositions of BSW are listed in Table 3, used in this work as the pore water infiltrating through the concrete mortar and compacted bentonite. The chemicals were in analytical grade with purity higher than 99%, meanwhile, all the reagents were prepared with distilled water (DSW).

2.2. Experimental device

To simulate the interaction of site water, degraded concrete, and compacted bentonite, the experimental mock-up device was designed. In this work, tests #1, #2, and #3 were carried out to observe the reactions of compacted GMZ bentonite with concretes at early, middle, and evolved degradation stages during the infiltration of BSW, respectively. The initial solution flows through the concrete and bentonite in turn, simulating the seepage path in an HLW repository. The schematic view of the concrete/bentonite interface mock-up device is shown in Fig. 2a, and the picture of each instrument after installation is presented in Fig. 2b. The testing setup of the site water-concrete-compact bentonite

Table 2
Design mix ratios of concrete mortar at different degradation stages.

| Sample | #1 | #2 | #3 |
|--------------------------|------------------------------|------------------------------------|---------------------------|
| Cement degradation stage | Young | Middle | Evolved |
| Formula | Quartz-sand : cement : water | Quartz-sand : (cement+CaO) : water | Quartz-sand : CaO : water |
| Ratio | 3.5 : 0.8 : 0.5 | 2 : (0.75 + 0.25) : 1.75 | 2 : 1 : 1.75 |

Table 3
Soluble salts and their concentrations in the Beishan site water (BSW).

| Content | Concentration (mg/L) |
|---------------------------------|----------------------|
| NaCl | 0.86 |
| Na ₂ SO ₄ | 4.24 |
| CaCl ₂ | 0.81 |
| MgCl ₂ | 1.83 |
| KCl | 0.12 |

system includes the mock-up device of the concrete-bentonite interface, the solution control device, and the swelling measuring device.

2.2.1. Mock-up device of concrete-bentonite

It mainly includes a base, a sleeve, a solution chamber, a concrete sample ring, a bentonite sample ring, a porous stone, a sealing ring, a piston, etc. To maintain the sealing, thermal insulation, and corrosion resistance of the setup, the units of mock-up devices are made of stainless steel and Teflon material. The solution chamber, concrete sample, and bentonite sample are placed closely in the sleeve from bottom to top. In order to ensure the sealing performance of the device during the injection, sealing rings are placed at the connection positions.

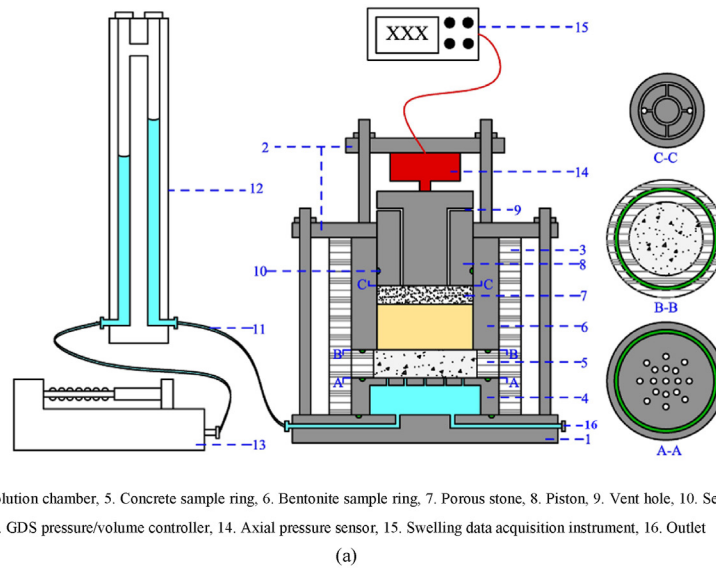
2.2.2. Solution control and swelling measuring devices

It mainly includes a pressure/volume controller, conduits, a water-solution converter, a water injection base, and a solution chamber for the solution control system. The pressure/volume controller can provide external experimental conditions such as constant water injection or constant pressure, connected with a water-solution converter by polytetrafluoroethylene pipes with its injected water volume and pressure of real-time seepage recorded by a computer. Since the pressure/volume controller is a precision instrument, a water-solution converter is designed to prevent it from being corroded by chemical solutions. The water-solution converter contains three liquids: the distilled water, the chemical solution, and the silicone oil to separate the former two, as shown in Fig. 2. The distilled water in the converter is connected to the pressure/volume controller, and the other end is connected to the base providing chemical solutions through the conduits (polytetrafluoroethylene pipes). The swelling measuring device is composed of an axial pressure sensor and a data acquisition instrument. When the solution infiltrates through the concrete into bentonite, the hydration of bentonite will induce a swelling process, which would be recorded by a data acquisition instrument via the axial pressure sensor.

2.3. Experimental procedures

2.3.1. Sample preparation

2.3.1.1. Concrete mortar preparation. The concrete samples #1 and #2 were placed in a Teflon ring with an inner diameter of 60 mm and a height of 15 mm. The diameter is larger than that of bentonite samples to prevent the shrinkage gap caused by hardening. For



1. Base, 2. Upper cap, 3. Sleeve, 4. Solution chamber, 5. Concrete sample ring, 6. Bentonite sample ring, 7. Porous stone, 8. Piston, 9. Vent hole, 10. Seal ring, 11. polytetrafluoroethylene pipe, 12. Water-solution converter, 13. GDS pressure/volume controller, 14. Axial pressure sensor, 15. Swelling data acquisition instrument, 16. Outlet



Fig. 2. The experimental device of the mock-up test: (a) Schematic view of the experimental device; (b) Photograph of the test system.

concrete sample #3, the amount of curing shrinkage is small, and the sample is in good contact with the boundary. Concrete samples #3 with the inner diameter of 50 mm and 60 mm were both employed. They were considered parallel trials with similar results obtained in this study. To ensure high strength and permeability, the concrete mortar was thoroughly stirred in the Teflon ring, placed on filter paper during the preparation process, and then hardened for 28 d. The photo of concrete #2 is shown in Fig. 3, it can be seen that the mortar is porous and not dense.

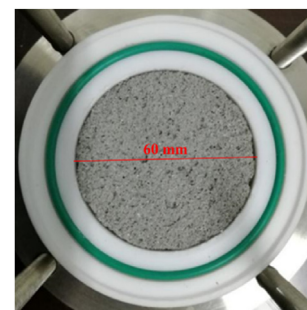


Fig. 3. Photo of concrete #2 used in this work.

2.3.1.2. Bentonite sample preparation. According to the preset dry density of 1.7 Mg/m^3 for GMZ bentonite, the bulk soil with the initial water content of 10.28% was calculated at 92.1 g for a specimen of $50 \text{ mm} \times 24 \text{ mm}$ (diameter \times height). To ensure the uniformity of compacted bentonites, the compaction process was carried out in three stages, each with a height of 8 mm. 1/3 GMZ bentonite powder was poured into the stainless-steel ring each time, and then slowly compressed at a displacement rate of 0.1 mm/min. After a stage of compaction, a 2–3 mm deep well grid was drawn on the surface of the sample to ensure adequate occlusion of the specimens at this stage and the next one. After the compaction, the samples were left in place for 1 h to ensure uniform structural adjustment. At last, the sample was unloaded at a displacement rate of 0.5 mm/min.

2.3.2. Experimental procedures

Firstly, the hardened concrete sample was placed in the Teflon ring. Then, put the whole device together in sequence as shown in Fig. 2a. The mock-up device was connected to the water-solution converter and the pressure/volume controller. The axial pressure sensor was installed. At last, the infiltration process was controlled by the pressure/volume controller with injection pressure kept at 200 kPa. Besides, the injection water in the stainless-steel solution chamber was collected regularly through the drainage port of the base. After that, the concentration of cations in the solution was

determined by an inductively coupled plasma source mass spectrometer (ICP, PerkinElmer, America). After the mock-up tests, the samples were taken out, and the soils at 6 mm, 12 mm, and 18 mm height away from the interface were cut out for water content and dry density measurements. The water content was obtained by drying the soils in an oven at 105 °C for 24 h. The dry density of samples was measured by using the wax sealing method. All the data were recorded with the averages in triplicate.

2.4. Characterization

After the mock-up tests, some samples in the middle part were washed with ethyl alcohol 3 times. The suspension was subjected to centrifuge for 4 min at 7000 r/min. After that, the purified samples were dried in an oven at a temperature of 50 °C. Finally, the dried soils were ground finely and screened through a 200-mesh sieve to obtain powders for mineralogy characterizations. The GMZ bentonite characterization was conducted using the random powder by Fourier infrared spectroscopy (FTIR) (Model Nicolet Avatar 360, USA) and X-ray diffraction (XRD) (Model APD-10, Philips, Netherlands). The GMZ bentonite samples were pretreated in pressed KBr pellets to determine their functional groups in FTIR tests. In each spectrum, 32 scans were collected with a resolution setting at 2 cm^{-1} . The scanning wavelength range is 400–4000 cm^{-1} at room temperature. The bentonites were characterized with $\text{CuK}\alpha$ (0.15418 nm) radiation from 5° to 45° in XRD tests with a scanning rate of 2°/min. The XRD pattern was identified based on the PDF2 database (ICDD 2013).

3. Results and analysis

3.1. Sample observations after mock-up tests

After the mock-up tests, the bentonite specimens were taken out of the metallic cells (Fig. 4). Due to the tight connection between the bentonite sample and the units (Bentonite sample ring, Piston, and Seal ring in Fig. 2a), it was failed to take sample #2 out. From Fig. 4, two sides of the concrete/bentonite interface in tests #1 and #3 are shown, that is the top surface of concrete and the bottom surface of bentonite, respectively. Due to the uneven surface of concrete #1, the bottom surface of bentonite is also irregular, and a ring of bentonite colloids is formed on the edge of sample #1. The bottom surface of sample #3 seems flatter and more regular. It can be observed that the cement or lime component from the mortars has entered the underside of bentonite samples. Additionally, after removing the uneven undersurface, the bottom of bentonite is displayed in Fig. 4c and f. It is found that the bottom and longitudinal sections of samples are distinctly different. The brittleness of sample #1 is higher than that of sample #3, which can be confirmed by the flatness and regularity of the soil notch in Fig. 4c and f. Besides, after the reactions of BSW-concrete-bentonite, the bottom color of sample #1 is dark green, and it reduces gradually with height. From the longitudinal section, the color transitions from dark green to yellow. The yellow with light green color in sample #1 is similar to the samples' color identified by Fernández et al. (2009, 2013) and the color of GMZ bentonite infiltrated by young cement water (YCW) on Sun et al. (2019). These features suggest that the reactions between bentonite and OPC might be similar to the reactions between YCW (pH 13) and bentonite, which reflects the rationality of using a strong alkaline solution (Na–K–OH type) to simulate the early degradation of concrete. In addition, the color of sample #3 is deep brown, which is also similar to that of bentonite in Evolved cement water (ECW) (Sun et al., 2019). There are some white spots on the bottom surface of bentonite and the longitudinal section near the interface, which

should be the hydrated lime.

The final dry density of bentonite samples (initial dry density of 1.7 Mg/m^3) after the reactions was also detected. Three soil samples were cut from the bottom to the top according to the height from the concrete-bentonite interface to measure the final dry density and water content. The results are shown in Fig. 5. It is seen from Fig. 5a that the dry density is lower than the initial value. It was observed by Dong (2020) that there is about 0.1 Mg/m^3 of density decrease in bentonite (with an initial dry density of 1.7 Mg/m^3) after hydration by distilled water during the constant volume tests, which is speculated due to the systematic error caused by space at the junction. In this work, it is more than 0.1 Mg/m^3 of density decrease, especially at the bottom side. From Fig. 4, the soil is found entering concrete pores, which should be one of the main reasons for the dry density loss. It makes sense that the dry density of the bentonite sample decreases from the top to the bottom. In addition, the dry density of sample #3 is higher than that of sample #1, suggesting that the reactions in sample #1 are more intense than those in sample #3. The final dry density was also measured by Liu et al. (2020) while the GMZ bentonite was subjected to 0.1–1 mol/L NaOH solutions for 27 d, ranging from 1.525 Mg/m^3 to 1.614 Mg/m^3 . All these results indicate that the chemical conditions have significant impacts on the dry density of bentonite.

The final water contents of compacted GMZ bentonite after reacting with concrete and BSW are presented in Fig. 5b. It can be observed from Fig. 5b that the water content of bentonite decreases from the bottom to the top according to the height from the concrete-bentonite interface for both samples #1 and #3, turning an opposite trend of the dry density. The water content in sample #1 is lower than that in sample #3. Under normal circumstances, the water content of bentonite should be higher when its dry density is lower because its internal porosity is bigger in this case. However, when comparing the two samples, sample #1 has a lower dry density and a lower water content at the same time in Fig. 5. It suggests that the materials of sample #1 and sample #3 differ from each other, and the water retention capacity of sample #1 is lower than that of sample #3 (Sun et al., 2019).

3.2. Swelling pressure of bentonite in mock-up tests

The swelling pressure development in compacted GMZ bentonite infiltrated by BSW with and without contact with concretes is shown in Fig. 6. It is observed that the maximum swelling pressure of pure bentonite without contact with concrete is 4.9 MPa (Sun et al., 2018), which is higher than that of 4.5 MPa for the bentonite in the mock-up tests. In addition to the variable of concrete, the height of bentonite is 10 mm in the former and 24 mm in the latter, both of which may affect the swelling of bentonite. During the hydration process of bentonite infiltrated by BSW, the swelling pressure presents a “double-peak” structure, which is in agreement with the results reported by Chen et al. (2019) and Sun et al. (2018). The swelling pressure of GMZ bentonite increases rapidly and reaches its first peak with the value of about 4 MPa after around one day's hydration in the mock-up tests. It takes the shortest time for the swelling pressure of pure bentonite to reach its first peak and the longest one for that of sample #2. Associating with the findings from Sun et al. (2018), the effect of chemical pore solutions on compacted GMZ bentonite is negligible in the initial hydration process. The possible reason is that the penetration path of the liquid affects the swelling rate of bentonite. Additionally, mortar #2 may have a higher strength and lower permeability due to the hydration reactions in the cement-lime mixture (Corinaldesi et al., 2015), which can slow down the rate of water infiltration and the hydration process of bentonite. It was also in agreement with the findings from Ince (2015) that the hydrated lime mixes may



Fig. 4. The samples after mock-up tests. Sample #1: (a) Top surface of the concrete; (b) Bottom surface of the specimen; (c) Bottom and longitudinal sections. Sample #3: (d) Top surface of the concrete; (e) Bottom surface of the specimen; (f) Bottom and longitudinal sections.

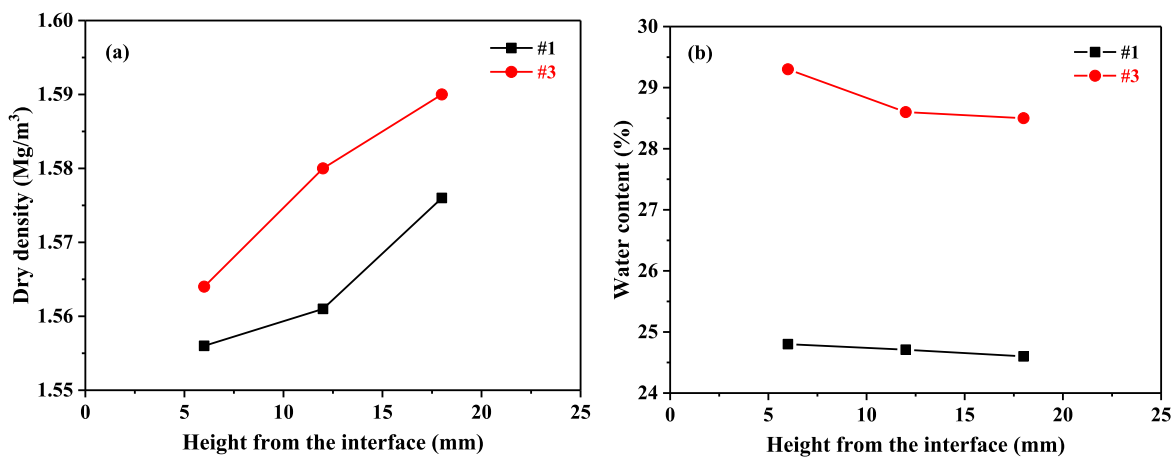


Fig. 5. The dry density and water content of samples at different positions: (a) Dry density; (b) Water content.

influence the water transport characteristics of the cement mortar.

It is also observed that after reaching the second peak, the swelling pressure of bentonite in contact with concrete decreases with the extension of time. In order to quantitatively describe the reduction of bentonite swelling pressure in the concrete/bentonite system, the decay rate (v) of swelling pressure is calculated according to the equation from Sun et al. (2020), as follows:

$$v = \frac{P_1 - P_2}{t_1 - t_2} \tag{1}$$

where P_1 and P_2 are the swelling pressure of samples at time t_1 and t_2 , respectively. The calculated swelling pressure decay rates are 1.35 kPa/d in sample #1, 1.26 kPa/d in sample #2, and 1.35 kPa/d in

sample #3, respectively.

3.3. Permeability of bentonite in mock-up tests

The fluids are injected from the bottom of the mock-up device under pressure controlled by a pressure/volume controller. In this permeability test, the injection pressure was set at 200 kPa. While keeping the pressure constant, the water volume injected into the concrete-bentonite samples over time was recorded. The flux rate ($\Delta Q/\Delta t$) was calculated as shown in Fig. 7. The permeability is obtained in sample #1 > sample #3 > sample #2. The permeability of the concrete sample is significantly greater than that of bentonite, as evidenced by the results presented in Fig. 6. It takes approximately 15 min for BSW to infiltrate through the concrete, interact

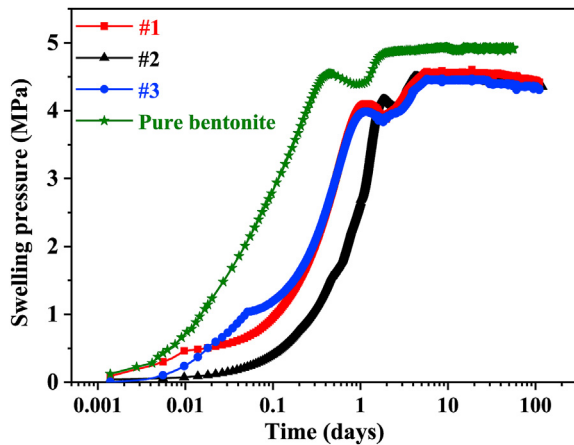


Fig. 6. Swelling pressure development in samples contacting with/without concrete under the infiltration of BSW.

with the bentonite, and induce its swelling. Thus, it is neglected in the analysis. From Fig. 7, it is also found that the permeability of bentonite samples in the three devices decreases slowly with time. The reasons for the permeability decrease may be: (1) The complex chemical reactions between bentonite and the pore solution; (2) Some minerals in bentonite dissolve and clog pores (Sun et al., 2019); (3) Some bentonite particles disperse into the solution forming a colloid solution increasing the water viscosity. This can be confirmed by the findings of Yoon et al. (2022) which demonstrate that the change in the hydraulic properties of bentonite can be related to the change in the kinematic viscosity of the permeant. Compared with the other permeability results in GMZ bentonite (1.7 Mg/m³) by Ye et al. (2013, 2014) and Chen et al. (2021), the flux rate is also highest at the beginning and then decreases gradually to a stable seepage state, which takes about 16 d to reach a stable state. In the concrete-bentonite system, it takes about 120 d to reach a relatively stable state for GMZ bentonite. This implies that the bentonite required a considerable period of time to reach its chemical equilibrium state in the system (Katsumi et al., 2008), which illustrates the complexity and persistence of internal reactions.

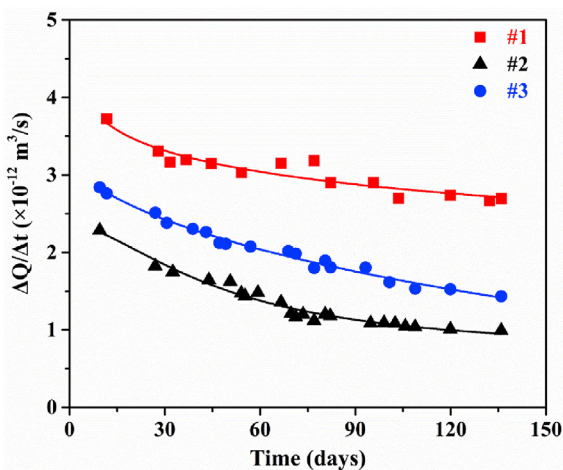


Fig. 7. Evolution of fluxes over time in concrete-GMZ bentonite interaction system.

It was reported that the saturated hydraulic conductivity of GMZ bentonite (1.7 Mg/m³) is about 1.5×10^{-13} – 2×10^{-13} m/s when injected by DSW under the head pressure of 1 MPa (Ye et al., 2014; Chen et al., 2021), which is much lower than the values obtained in this work. It also indicates that the injection pressure influences the permeability of compacted bentonite significantly. Fig. 8 presents the flux rate versus the hydraulic gradient for GMZ bentonite of 1.7 Mg/m³ at the infiltration time of 16 d. From Fig. 8, it can be seen that the flux rate of GMZ bentonite differs with the head pressure and solution types. The higher the pressure is, the larger the flux rate is within the scope of these tests. Under the same DSW conditions, the head pressure of 1 MPa is 50 times of 20 kPa, while the corresponding flow rate in bentonite is 5.5 times the latter case (Fig. 8). According to Darcy's law, hydraulic conductivity is independent of osmotic pressure (hydraulic gradient), which is considered as a material constant. However, for the same material (GMZ bentonite of 1.7 Mg/m³) and the sample area (with a diameter of 50 mm), the change in flow rate and pressure is not proportional. It can be deduced that the high hydraulic gradient may induce the material or seepage path change resulting in a reduction in the hydraulic conductivity. The specific reason was inferred as internal erosion or microstructure clogging in bentonite (Pusch et al., 2011), or the material compression caused by the high gradient (Al-Taie et al., 2014).

3.4. Geochemical evolution of pore water

As reported, the cations released in the early stage of concrete degradation are mainly K⁺ and Na⁺, while in the evolved stage it is mainly Ca²⁺ (Berner, 1992; Savage et al., 2002; Fernández et al., 2009). The cations released in the middle stage should have the characteristics of both the two stages. When the solution infiltrates through the concrete-bentonite system, it reacts with cement and bentonite, which will also affect its chemical compositions in turn. In order to observe the chemical evolution of solution compositions during the interaction, the concentrations of main cations and the pH of output solutions were measured. The initial BSW and the solutions after the reaction of BSW-concrete-bentonite were analyzed with the concentration of cations detected by ICP tests. The results are shown in Fig. 9. It can be seen from Fig. 9a that the concentration of K⁺ in test #1 after reactions in the BSW-young concrete-bentonite system increases significantly compared with that in the initial water. This result is consistent with the conclusion

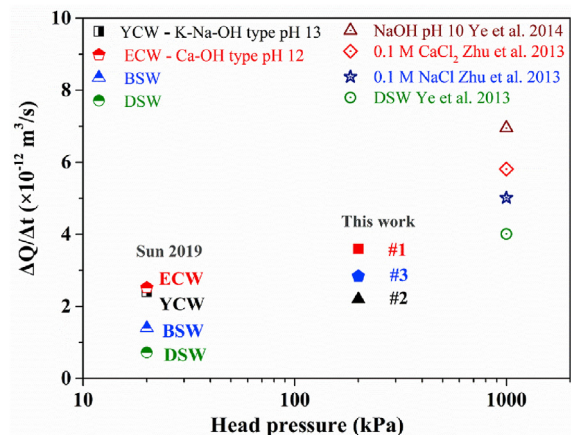


Fig. 8. The flux versus the hydraulic gradient for GMZ bentonite of 1.7 Mg/m³.

that K^+ is the main cation released in the early stage of concrete degradation (Bernier, 1992; Fernández et al., 2006). The concentration of K^+ in test #2 increases significantly in the first 100 d, and then in the next 100 d–240 d. It is close to that in the initial BSW. The K^+ concentration in test #3 is quite different from those in the other two tests, which is lower than that in the initial solution. Considering that concrete #3 is lime mortar, which does not contain K^+ , it can be inferred that the reason for the decrease of K^+ may be that K^+ from the solution was absorbed by the bentonite

and the hydrated lime. Fig. 9b and c presents the concentrations of Mg^{2+} and Ca^{2+} in the solutions. The concentrations of Mg^{2+} and Ca^{2+} from the three systems are all lower than their initial concentrations, suggesting that Mg^{2+} and Ca^{2+} are consumed from the pore water. Different from K^+ , the contents of Mg^{2+} and Ca^{2+} in sample #3 are higher than those in tests #2 and #1. It may be attributed to the reasons that: (1) The evolved concrete releases more Ca^{2+} during the interactions, so there will be more Ca^{2+} in the solution, and this leads to less Mg^{2+} reacting with bentonite; (2)

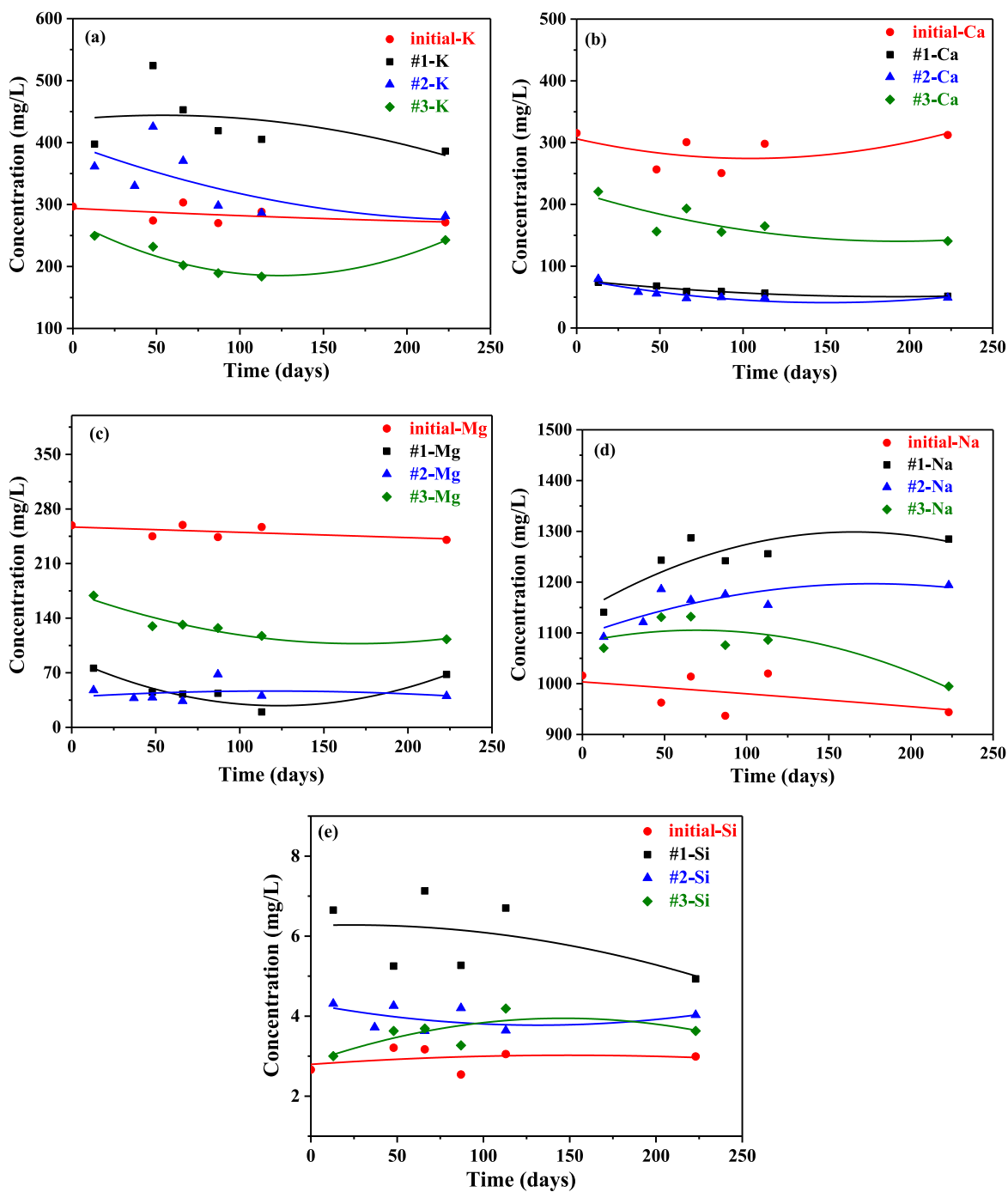


Fig. 9. Evolution of cation content in each case. (a) Concentration of K; (b) Concentration of Ca; (c) Concentration of Mg; (d) Concentration of Na; (e) Concentration of Si.

The hydrated cement in concretes #1 and #2 adsorbs more Mg^{2+} and Ca^{2+} than hydrate lime resulting in more consumptions of these cations. From Fig. 9d and e, both of Na^+ and Si^{4+} concentrations in the solutions present a significant increase compared with those in BSW. The order of Na^+ and Si^{4+} contents in different conditions follows test #1 > #2 > #3 > BSW. Because the main composition of concrete #3 is quartz and $Ca(OH)_2$, it does not contain Na and Si. Therefore, Na and Si in test #3 should come from the reactions between bentonite and solutions. The more Na and Si in tests #1 and #2 than those in test #3 should be due to the presence of Portland cement.

The average concentrations of cations (K, Na, Ca, Mg, Si) in tests #1, #2, #3, and initial BSW are summed up, respectively, as shown in Fig. 10. It is found that the cation content in test #1 is the highest, followed by that in the initial BSW. The one in test #2 is the lowest. The reason for the minimum cations in test #2 may be that the hydration process in the quicklime-cement mixture during the concrete preparation generates more stable substances. While interacting with BSW and bentonite, these substances not only reduce the release of chemical components but also absorb some chemical components from outside.

The pH of BSW and solutions from tests #1, #2, and #3 were measured periodically, as shown in Fig. 11. The pH of the initial BSW is relatively stable at about 6.9. It is found that the solutions from test #3 have the highest pH, which is about 8 in the first 120 d and 7.5 in the next days with a decreasing tendency. This should be due to the limited amount of concrete that cannot provide a stable Ca–OH component with time. It is in agreement with the study by Mosser-Ruck and Cathelineau (2004), in which a decrease of pH is observed with a final pH ranging from 7.1 to 8 after Na-, Ca-smectite reacted with solutions (pH 10) mixed by KCl (3 mol/L) and KOH. Moreover, the pH of solutions from test #1 is slightly higher than the pH of BSW. The pH of solutions in test #2 (about 6.5) is different from the above two cases, which is lower than the pH of the initial BSW. It can be drawn that the hydroxide is consumed most within this system.

3.5. Sample characterization after mock-up tests

The FTIR spectra of GMZ bentonite before and after the interaction with concretes are presented in Fig. 12 in the range of 400–4000 cm^{-1} . The broad bands at 3621 cm^{-1} and 3442 cm^{-1} represent the O–H stretching vibration of the Si–OH group and the H–OH vibration of water molecules (Sun et al., 2020). The band at 1643 cm^{-1} reflects an overtone of the bending vibration of water. The peak at 1035 cm^{-1} is due to the Si–O stretching vibration (Hu

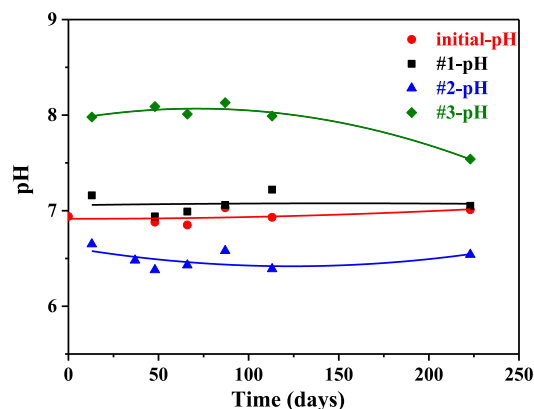


Fig. 11. The pH evolution of each solution.

et al., 2010), which is the characteristic peak of bentonite representing the anti-symmetric stretching vibration of silica oxygen tetrahedron. It indicates that the main component of GMZ bentonite is montmorillonite. According to the Beer-Lambert law, the absorbances of raw GMZ bentonite, bentonite samples #1 and #3 are almost the same, which can be estimated that the content of montmorillonite in the three kinds of GMZ bentonite is similar. In addition, the intensity of reacted bentonite in samples #1 and #3 changes obviously compared with that of raw bentonite.

The XRD patterns of raw GMZ bentonite, sample #1, and sample #3 are presented in Fig. 13. The peaks marked as M are characteristic of montmorillonite. From Fig. 13, it can be observed that after interactions between bentonite and concrete with the infiltration of BSW, the (001) peaks of montmorillonite shift. A diffraction peak appears at 6.04° corresponding to the typical diffraction peak of montmorillonite in raw GMZ bentonite. From Bragg's Law, it could be determined that the interlayer spacing is 1.46 nm. The basal spacing (001) of montmorillonite in GMZ bentonite turns to 1.53 nm in GMZ bentonite from sample #1, which means that after the interaction, the montmorillonite layers present a little bit larger pore structure and layer spacing. It indicates that fewer monovalent cations occur in the crystal layer of GMZ bentonite. For the bentonite in sample #3, the basal spacing (001) is 1.37 nm. The peaks of montmorillonite at 19.71° (0.45 nm) and 34.74° (0.258 nm) change and become rough. In summary, according to the XRD results, the main reaction in GMZ bentonite is the cation

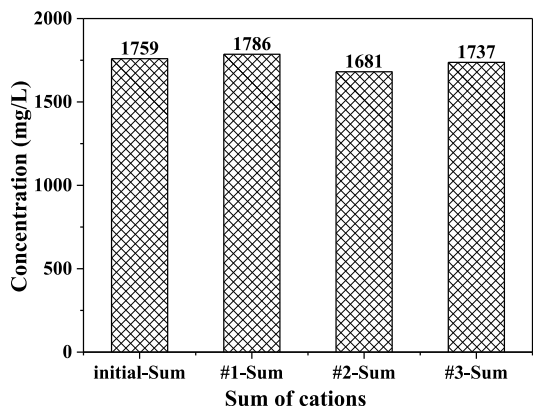


Fig. 10. Comparison of the total content of cations in each solution.

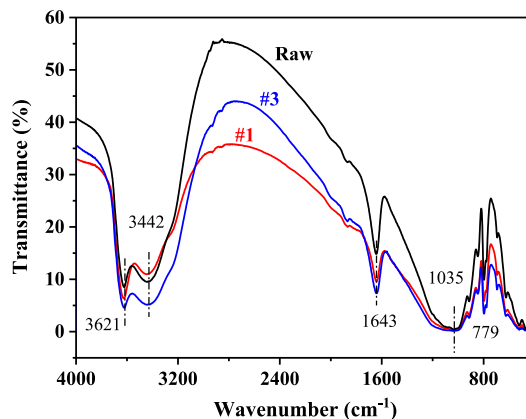


Fig. 12. FTIR spectra of GMZ bentonites.

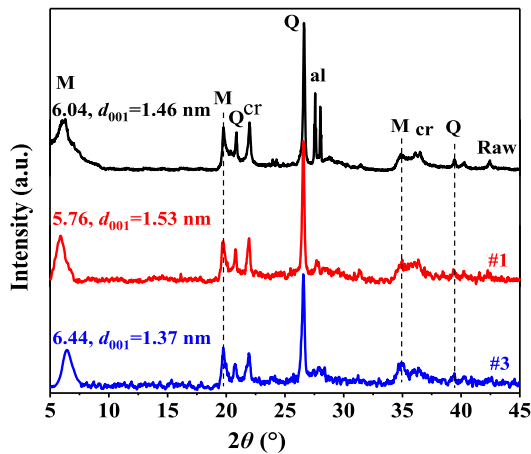


Fig. 13. XRD patterns of GMZ samples (M: montmorillonite; Q: quartz; cr: cristobalite; al: albite).

exchange reaction of montmorillonite. Besides, the albite peaks at 27.57° (0.323 nm) and 28.00° (0.318 nm) in raw bentonite disappeared in the samples after the mock-up tests. So, it can be drawn that albite dissolves during the test, which is in agreement with the findings from Gruber et al. (2019) that the albite dissolution occurs in synthetic NaCl solutions at pH 5–8.25 at 25 °C.

4. Discussions

4.1. The reactions in the BSW-concrete-bentonite system

The total change of cation contents from the interaction of 230 d is shown in Table 4. It can be found that a significant loss of Mg and Ca takes place in the three tests. Even in sample #3, the concrete was made of CaO, the content of Ca was also found a decrease. In addition, the increase of Na, K (except in the case of test #3), and Si is observed in the mock-up tests. The releasing content of Si and Na from the site water-concrete-bentonite system follows the order of #1 > #2 > #3. It indicates that the releasing Si and Na is dependent on the concrete type. It is obvious that the divalent cation is consumed and the monovalent cation is released in the mock-up system. It is known that after hydration, the main products generated in the cement include portlandite (Ca(OH)₂ or CH), calcium (aluminat) silicate hydrates (C-(A)-S-H), calcium aluminate hydrates (C-A-H), and ettringite. In the lime mortar, CH is the hydration product. These hydrations have good sorptivity to cations, especially the C–S–H gels presenting a high specific surface area (Pan et al., 2015).

According to the typically competitive order of cation exchanges: Na⁺ < K⁺ < Mg²⁺ < Ca²⁺ (Mata Mena, 2003; Sun et al., 2018), the cation sorption or cation exchange onto the bentonite and hydrated concretes in the BSW-concrete-bentonite system also follows this order, which could partly explain the great loss of Ca and Mg in the solutions and the increase of Na and K at the same

Table 4
Total cation content changes.

| Test | Total cation content change (mg/L) | | | | |
|------|------------------------------------|------|-------|-------|------|
| | Na | K | Ca | Mg | Si |
| #1 | 1560 | 881 | −1366 | −1210 | 18.3 |
| #2 | 1075 | 319 | −1402 | −1236 | 6.5 |
| #3 | 596 | −404 | −702 | −717 | 3.8 |

time. In the case of test #3, the K contents fall, which may be attributed to the reactions between K₂SO₄ and lime. It was reported that because of the longer atomic radii, the bonds of K₂SO₄ are more likely to break and adsorb to the lime particles than Na₂SO₄, which induces an increase in transfer sorptivity (Ince, 2015). In addition, it was observed that syngenite (K₂Ca(SO₄)₂·H₂O) was forming in a cement : lime : sand mortar exposed to the K₂SO₄ solution (Gaze and Crammond, 2000). Besides, it was also found that the pH can drop from 12.3 to 6.5 when this mortar was exposed to MgSO₄ solutions due to the reaction between lime and MgSO₄, which is similar to the pH results in this work (test # 2) since the dominant ions of BSW are also Mg and SO₄^{2−}. It explains the low alkalinity pH in tests #1 and #3 as well.

As to the effect of concrete mortar on bentonite, it was reported that the addition of cement (or lime) to clays triggers a cascade of reactions, which includes hydration reaction, cation exchange, pozzolanic reaction, etc., generating products and inducing flocculation and agglomeration of soil (Nelson and Miller, 1992; Abbey et al., 2019). Among the reactions, the pozzolanic reactions would consume the clay minerals (montmorillonite) from bentonite. Associated with the increasing brittleness and lower water content of sample #1 (see Figs. 4c and 5b), it can be deduced that the cementitious compounds filling into the compacted bentonite have impacts on both the material and behavior of bentonite. It is in agreement with the findings from Abbey et al. (2019) that the inclusion of cement (5% or 8%) reduces the plasticity index and swelling pressure of the kaolinite-bentonite mixed clays.

4.2. The macro-performance degradation of bentonite

The XRD results indicate an albite dissolution taking place in the systems (see Fig. 13), which would lead to an increase in Si concentration (Gruber et al., 2019). Additionally, it was reported by Rozalén et al. (2008) that the concentration of Si increases in the smectite dissolution experiments with pH around 6–8. From Fig. 9 and Table 4, it is shown that the increment of total Si is the smallest, which suggests the dissolution reactions are not dramatic. The altered macro-performance of bentonite might be partly due to the interactions in the BSW-concrete-bentonite system. Compared with the property of bentonite infiltrated by BSW with the absence of concrete, the swelling pressure decays in this work and the permeability of the samples increases. These results indicate that the direct contact of concrete and bentonite has an obvious effect on the properties of bentonite. The evidence observed in Fig. 4 shows that bentonite enters into the concrete pores and forms colloids at the interface. It can be deduced that the decrease in dry density in bentonite samples should be partly due to the soil dispersion during the infiltration. Additionally, the different apparent morphology of samples indicates that the bentonite alteration varies with the type of concrete mortar (e.g. cement mortar or lime mortar). The lower water content and higher dry density loss in sample #1 suggest the significant effect of cement mortar. The higher the distance from the interface, the lower the water content of the sample, indicating that the water absorption of bentonite farther away from the water inlet end is affected. In summary, the uneven water content and the dry density loss of samples in the longitudinal direction may also be part of the reason for the swelling reduction of bentonite.

From Fig. 7, the order of flow rate is sample #1 > sample #3 > sample #2, which is consistent with the order of total cation content (see Fig. 10). That is, the permeability of GMZ bentonite increases when the chemical concentration of infiltration solutions increases. This phenomenon can be explained by the compression of the diffusion double layer when the chemical concentration of the permeated solution increases. This leads to the formation of

larger pores between soil particles, creating a wider seepage channel, and thus increasing the soil permeability (Castellanos et al., 2008).

It can be concluded from this work that the mineral dissolution and hydro-mechanical property degradation in bentonite occur under the conditions of strong alkali solutions and also when bentonite directly contacts with cement (or lime) mortar, even in groundwater with an approximate neutral pH. Besides, the bentonite dispersion at the interface should be taken into consideration, which can also affect the barrier performance of bentonite.

4.3. Limitations of this work and suggestions

As a preliminary experimental study, this work still has many shortcomings and many improvements need to be made. The overall test is easy to repeat, and the difficulty mainly lies in the sealing problem of each joint during the installation of setup. During the test, the vent hole above the sample was open, but the exudate could not be obtained for a long time due to the high density and low permeability of the bentonite. Moreover, the head pressure of 200 kPa is not a low level, however, the water content of bentonite at different heights is still uneven. These can be improved by adjusting the size of specimen and soil parameters such as initial dry density. In addition, this work only simulates the effects of concrete mortar on bentonite under the infiltration of neutral groundwater. In fact, in more extreme cases, mixed alkaline solution may induce more obvious alteration of bentonite. Therefore, more works are needed in this field to verify the engineering and mineralogical impact of concrete mortar on bentonite. It is also worth emphasizing that the results of cement-bentonite interactions were obtained under laboratory-scale conditions, and their applicability in this field remains to be further explored.

5. Conclusions

A mock-up device was designed to simulate an in situ interaction of concrete-bentonite under the infiltration of Beishan site water in a potential Chinese repository. The hydro-mechanical performance of compacted GMZ bentonite in the site water-concrete-bentonite system at different concrete degradation stages was studied. The chemical evolution of solution compositions and the sample characters after the mock-up interactions were also investigated. Based on the above results, the following main conclusions are drawn.

- (1) The swelling pressure of bentonite in the three devices decays slowly with time.
- (2) The flow rate of bentonite samples in tests #1, #2, and #3 takes more time to stabilize, and it is related to the total cation content of injections and affected by the head pressure.
- (3) After the reactions in the synthetic site water-concrete-bentonite system, the divalent cations (Ca and Mg) are consumed, the monovalent cations (Na and K) are released, and the Si content increases weakly. The cation exchange reaction is the dominant reaction in the system.
- (4) The dissolution of albite in bentonite was identified, and the bentonite dispersion at the interfaces was observed, which resulted in a dry density loss in bentonite affecting the barrier performance of bentonite.
- (5) The hydro-mechanical property degradation of bentonite takes place when it contacts with concrete mortar even under low alkaline conditions.

Declaration of competing interest

The authors declare that they have no known competing financial interests or personal relationships that could have appeared to influence the work reported in this paper.

Acknowledgments

The work was supported by the National Natural Science Foundation of China (Grant No. 42125701), the Innovation Program of Shanghai Municipal Education Commission (Grant No. 2023ZKZD26), Fund of the Shanghai Science and Technology Commission (Grant No. 22DZ2201200), Top Discipline Plan of Shanghai Universities-Class I and the Fundamental Research Funds for the Central Universities. Financial support from the International Post-Doc Fund of The Hong Kong Polytechnic University is greatly appreciated.

References

- Abbey, S.J., Eyo, E.U., Ng'ambi, S., 2019. Swell and microstructural characteristics of high-plasticity clay blended with cement. *Bull. Eng. Geol. Environ.* 79 (4), 2119–2130.
- Al-Taie, L., Pusch, R., Knutsson, S., 2014. Hydraulic properties of smectite rich clay controlled by hydraulic gradients and filter types. *Appl. Clay Sci.* 87, 73–80.
- Balmer, S., Kauffhold, S., Dohrmann, R., 2017. Cement-bentonite-iron interactions on small scale tests for testing performance of bentonites as a barrier in high-level radioactive waste repository concept. *Appl. Clay Sci.* 135, 427–436.
- Berner, U.R., 1992. Evolution of pore water chemistry during degradation of cement in a radioactive waste repository environment. *Waste Manag.* 12, 201–219.
- Castellanos, E., Villar, M.V., Romero, E., Lloret, A., Gens, A., 2008. Chemical impact on the hydro-mechanical behaviour of high-density febex bentonite. *Phys. Chem. Earth, Parts A/B/C* 33 (Suppl. 1), S516–S526.
- Chen, Y.G., Cai, Y.Q., Pan, K., Ye, W.M., Wang, Q., 2021. Influence of dry density and water salinity on the swelling pressure and hydraulic conductivity of compacted GMZ01 bentonite-sand mixtures. *Acta Geotech* 17, 1879–1896.
- Chen, Y.G., Sun, Z., Cui, Y.J., Ye, W.M., Liu, Q.H., 2019. Effect of cement solutions on the swelling pressure of compacted GMZ bentonite at different temperatures. *Construct. Build. Mater.* 229, 116872.
- Corinaldesi, V., Nardinocchi, A., Donnini, J., 2015. The influence of expansive agent on the performance of fibre reinforced cement-based composites. *Construct. Build. Mater.* 91, 171–179.
- Cuevas, J., Ruiz, A.I., Fernández, R., et al., 2016. Lime mortar-compacted bentonite-magnetite interfaces: an experimental study focused on the understanding of the EBS long-term performance for high-level waste isolation DGR concept. *Appl. Clay Sci.* 124–125, 79–93.
- Cuevas, J., Turrero, M.J., Torres, E., Fernández, R., Ruiz, A.I., Escribano, A., 2013. Long-term performance of engineered barrier systems PEBS. Laboratory tests at the interfaces: results of small cells with mortar-bentonite-magnetite. https://igdtp.eu/wp-content/uploads/2018/04/D2_3_3_2.pdf.
- Dauzeres, A., Achiedo, G., Nied, D., Bernard, E., Alahache, S., Lothenbach, B., 2016. Magnesium perturbation in low-pH concretes placed in clayey environment solid characterizations and modeling. *Cement Concr. Res.* 79, 137–150.
- Dauzeres, A., Le Bescop, P., Sardini, P., Cau Dit Coumes, C., 2010. Physico-chemical investigation of clayey/cement-based materials interaction in the context of geological waste disposal: experimental approach and results. *Cement Concr. Res.* 40 (8), 1327–1340.
- Dolder, F., Mäder, U., Jenni, A., Schwendener, N., 2014. Experimental characterization of cement-bentonite interaction using core infiltration techniques and 4D computed tomography. *Phys. Chem. Earth (Parts A/B/C)* 70–71, 104–113.
- Dong, X.X., 2020. Hydraulic and Mechanical Properties of Densely Compacted GMZ Bentonite and its Assembled Interface. PhD Thesis. Tongji University, Shanghai, China, pp. 40–43 (in Chinese).
- Faucon, P., Adenot, F., Jacquinet, J.F., Petit, J.C., Cabrillac, R., Jorda, M., 1998. Long-term behavior of cement pastes used for nuclear waste disposal: review of physico-chemical mechanisms of water degradation. *Cement Concr. Res.* 28 (6), 847–857.
- Fernández, R., Cuevas, J., Mäder, U.K., 2010. Modeling experimental results of diffusion of alkaline solutions through a compacted bentonite barrier. *Cement Concr. Res.* 40 (8), 1255–1264.
- Fernández, R., Cuevas, J., Sánchez, L., Vigil de la Villa, R., Leguey, S., 2006. Reactivity of the cement-bentonite interface with alkaline solutions using transport cells. *Appl. Geochem.* 21 (6), 977–992.
- Fernández, R., Mäder, U., Rodríguez, M., Vigil de la Villa, R., Cuevas, J., 2009. Alteration of compacted bentonite by diffusion of highly alkaline solutions. *Eur. J. Mineral* 21 (4), 725–735.
- Fernández, R., Villa, R., Ruiz, A.I., García, R., Cuevas, J., 2013. Precipitation of chlorite-like structures during OPC porewater diffusion through compacted bentonite at 90 °C. *Appl. Clay Sci.* 83 (84), 357–367.

- Fernández, R., Torres, E., Ruiz, A.I., et al., 2017. Interaction processes at the concrete-bentonite interface after 13 years of FEBEX-Plug operation. Part II: bentonite contact. *Phys. Chem. Earth, Parts A/B/C* 99, 49–63.
- Gaze, M.E., Crammond, N.J., 2000. The formation of thaumasite in a cement:lime:sand mortar exposed to cold magnesium and potassium sulfate solutions. *Cem. Concr. Compos.* 22, 209–222.
- Glasser, F.P., 2001. Mineralogical aspects of cement in radioactive waste disposal. *Mineral. Mag.* 65 (5), 621–633.
- Glasser, F.P., Atkins, M., 1994. Cements in radioactive waste disposal. *Mater. Res. Bull.* 12, 33–39.
- Gruber, C., Harlavan, Y., Pousty, D., Winkler, D., Ganor, J., 2019. Enhanced chemical weathering of albite under seawater conditions and its potential effect on the Sr ocean budget. *Geochem. Cosmochim. Acta* 261, 20–34.
- Guo, Y.H., Li, Y.W., Wang, H.L., Su, R., Liu, S.F., Zong, Z.H., 2010. Study on regional hydrogeochemical characteristics of Beishan area—the preselected area for China's high level radioactive waste repository. In: *Proceedings of the Third Conference on Underground Disposal of the Waste*, pp. 19–24 (in Chinese).
- Guo, Y.H., Yang, T.X., Liu, S.F., 2001. Hydrogeological characteristics of Beishan preselected area, Gansu province for China's high-level radioactive waste repository. *Uranium Geol.* 3 (17), 184–189.
- Heath, T.G., Hunter, F.M.I., 2012. Calculation of Near-Field pH Buffering: Effect of Polymer Encapsulant. Serco Report, SA/ENV-0909, Issue 2.
- Hu, J., Xie, Z., He, B., et al., 2010. Sorption of Eu(III) on GMZ bentonite in the absence/presence of humic acid studied by batch and XAFS techniques. *Sci. China Chem.* 53 (6), 1420–1428.
- Ince, C., 2015. Possible role of simple ionic solutions on the water transport kinetics and mechanical properties of hydrated lime mortars. *J. Mater. Civ. Eng.* 27 (3), 04014124.
- Katsumi, T., Ishimori, H., Onikata, M., Fukagawa, R., 2008. Long-term barrier performance of modified bentonite materials against sodium and calcium permeant solutions. *Geotext. Geomembranes* 26 (1), 14–30.
- Karland, O., Olsso, S., Nilsson, U., et al., 2007. Experimentally determined swelling pressures and geochemical interactions of compacted Wyoming bentonite with highly alkaline solutions. *Phys. Chem. Earth, Parts A/B/C* 32 (1–7), 275–286.
- Kaufhold, S., Dohrmann, R., Ufer, K., 2020. Determining the extent of bentonite alteration at the bentonite/cement interface. *Appl. Clay Sci.* 186, 105446.
- Lalan, P., Dauzères, A., De Windt, L., et al., 2016. Impact of a 70 °C temperature on an ordinary Portland cement paste/claystone interface: an in situ experiment. *Cement Concr. Res.* 83, 164–178.
- Lehikoinen, J., 2009. Bentonite-Cement Interaction—Preliminary Results from Model Calculations. Working Report, 2009-37, Finland.
- Liu, L.N., Chen, Y.G., Gao, W.S., 2023. Effect of multiple-ion interaction on the swelling pressure of compacted Gaomiaozi (GMZ) bentonite. *Bull. Eng. Geol. Environ.* 82, 90.
- Liu, L.N., Chen, Y.G., Ye, W.M., Cui, Y.J., Wu, D.B., 2020. Swelling pressure deterioration of compacted GMZ bentonite and its structural damage under heat combined with hyperalkaline conditions. *Geomechanics Geoenviron. Eng.* 17 (1), 297–308.
- Mata Mena, C., 2003. Hydraulic Behaviour of Bentonite Based Mixtures in Engineered Barriers: the Backfill and Plug Test at the Äspö HRL (Sweden). PhD Thesis. Universitat Politècnica de Catalunya, Barcelona, Spain, pp. 35–49.
- Meyer, Th, Herbert, H.J., 1999. The long-term behaviour of cemented materials in highly saline solutions. FZK Karlsruhe. In: *Proceeding of the 2nd Geochemistry Workshop*. Speyer, Germany.
- Mon, A., Samper, J., Montenegro, L., Naves, A., Fernández, J., 2017. Long-term non-isothermal reactive transport model of compacted bentonite, concrete and corrosion products in a HLW repository in clay. *J. Contam. Hydrol.* 197, 1–16.
- Mosser-Ruck, R., Cathelineau, M., 2004. Experimental transformation of Na, Ca-smectite under basic conditions at 150 °C. *Appl. Clay Sci.* 26 (1–4), 259–273.
- Nakayama, S., Sakamoto, Y., Yamaguchi, T., et al., 2004. Dissolution of montmorillonite in compacted bentonite by highly alkaline aqueous solutions and diffusivity of hydroxide ions. *Appl. Clay Sci.* 27 (1–2), 53–65.
- Nelson, J.D., Miller, D.J., 1992. *Expansive Soils: Problems and Practice in Foundation and Pavement Engineering*. Wiley, New York, USA.
- Pan, Z., He, L., Qiu, L., et al., 2015. Mechanical properties and microstructure of a graphene oxide–cement composite. *Cem. Concr. Compos.* 58, 140–147.
- Pusch, R., 1979. Highly compacted sodium bentonite for isolating rock-deposited radioactive waste products. *Nucl. Technol.* 45 (2), 153–157.
- Pusch, R., Yong, R.N., Nakano, M., 2011. *High-level Radioactive Waste (HLW) Disposal*. WIT Press, Southampton, UK.
- Qian, L.X., 2007. A Fundamental Study of GMZ Bentonite as Buffer Material in Deep Geological Disposal for High-Level Radioactive Waste (China). PhD Thesis. Tongji University, Shanghai, China, pp. 71–72 (in Chinese).
- Rozalén, M.L., Huertas, F.J., Brady, P.V., Cama, J., García-Palma, S., Linares, J., 2008. Experimental study of the effect of pH on the kinetics of montmorillonite dissolution at 25 °C. *Geochem. Cosmochim. Acta* 72 (17), 4224–4253.
- Savage, D., 1997. Review of the Potential Effects of Alkaline Plume Migration from a Cementitious Repository for Radioactive Waste. Technical Report, No. 60. Environment Agency, UK.
- Savage, D., Noy, D., Mihara, M., 2002. Modelling the interaction of bentonite with hyperalkaline fluids. *Appl. Geochem.* 17 (3), 207–223.
- Sun, Z., Chen, Y.G., Cui, Y.J., Xu, H.D., Ye, W.M., Wu, D.B., 2018. Effect of synthetic water and cement solutions on the swelling pressure of compacted Gaomiaozi (GMZ) bentonite: the Beishan site case, Gansu, China. *Eng. Geol.* 244, 66–74.
- Sun, Z., Chen, Y.G., Cui, Y.J., Ye, W.M., Chen, B., 2019. Effect of synthetic Beishan site water and cement solutions on the mineralogy and microstructure of compacted Gaomiaozi (GMZ) bentonite. *Soils Found.* 59 (6), 2056–2069.
- Sun, Z., Chen, Y.G., Cui, Y.J., Ye, W.M., Wang, Q., 2020. Swelling deformation of Gaomiaozi bentonite under alkaline chemical conditions in a repository. *Eng. Geol.* 279, 105891.
- Villar, M.V., Lloret, A., 2008. Influence of dry density and water content on the swelling of a compacted bentonite. *Appl. Clay Sci.* 39, 38–49.
- Ye, W.M., Chen, Y.G., Chen, B., Cui, Y.J., Wang, J., 2010. Advances on the knowledge of the buffer/backfill properties of heavily-compacted GMZ bentonite. *Eng. Geol.* 116, 12–20.
- Ye, W.M., Wan, M., Chen, B., Chen, Y.G., Cui, Y.J., Wang, J., 2013. Temperature effects on the swelling pressure and saturated hydraulic conductivity of the compacted GMZ01 bentonite. *Environ. Earth Sci.* 68 (1), 281–288.
- Ye, W.M., Zheng, Z.J., Chen, B., Chen, Y.G., Cui, Y.J., Wang, J., 2014. Effects of pH and temperature on the swelling pressure and hydraulic conductivity of compacted GMZ01 bentonite. *Appl. Clay Sci.* 101, 192–198.
- Yoon, Y., Anh, H.N., Rha, S., Kim, J.-S., Jo, H.Y., 2022. Hydraulic and physicochemical properties of dense thin bentonite layers permeated with variably mixed alkaline solutions of KOH and CaCl₂ at various temperatures (25–75 °C) for 3 years. *Geotext. Geomembranes* 50 (3), 521–534.



Yonggui Chen is a professor in the School of Civil Engineering, Tongji University, Shanghai, China. He received his BEng, MSc, and PhD from Central South University in Hunan Province, China, in 2004. He has long-time research experience in unsaturated soils, geo-environmental engineering, urban engineering geology, and contaminated soil. He has been awarded the 14th Youth Geological Science and Technology Award of China Geological Society; the National Science Fund for Outstanding Young Scholars (2014); First prize of the Natural Science Award of the Ministry of Education, China (2018); the National Science Fund for Distinguished Young Scholars (2021). He has published over 150 international journal papers and 3 industry standards in his research areas.